Electronic Supplementary Material (ESI) for Journal of Materials Chemistry A.
This journal is © The Royal Society of Chemistry 2017

Supporting Information for

A Stable Two-Electron-Donating Phenothiazine for Application in Nonaqueous Redox Flow Batteries

Jeffrey A. Kowalski,[a,b] Matthew D. Casselman,[c] Aman Preet Kaur,[c] Jarrod D. Milshtein,[a,d] Corrine F. Elliott,[c] Subrahmanyam Modekrutti,[c] N. Harsha Attanayake[c], Naijao Zhang,[c] Sean R. Parkin,[c] Chad Risko,[c,e] Fikile R. Brushett,[*,a,b] Susan A. Odom[*,c]

[a] Joint Center for Energy Storage Research, USA
[b] Department of Chemical Engineering, Massachusetts Institute of Technology, Cambridge, MA 02139, USA
[c] Department of Chemistry, University of Kentucky, Lexington, KY 40506, USA
[d] Department of Materials Science and Engineering, Massachusetts Institute of Technology, Cambridge, MA 02139, USA
[e] Center for Applied Energy Research, University of Kentucky, Lexington, KY 40511, USA

I. Synthesis

Materials. Hexanes, diethyl ether, and ethyl acetate were Macron-brand, purchased from VWR. Copper (I) iodide (98%) and anhydrous acetonitrile (99.8%, extra dry) were purchased from Acros Organics. $NOBF_4$ (98%) was purchased from Alfa Aesar. Magnesium sulfate was purchased from Fisher Scientific. Anhydrous methanol (99.8%), anhydrous pyridine (99.8%), and sodium were purchased from Sigma-Aldrich. Propylene carbonate and LiTFSI (both battery grade) were purchased from BASF Corporation (Florham Park, NJ) and stored in an argon-filled glovebox. Silica gel (65×250 mesh) was purchased from Sorbent Technologies. ^1H and ^{13}C NMR spectra were obtained on Varian spectrometers in DMSO-d_6 from Cambridge Isotope Laboratories.

Synthesis of *N*-ethylphenothiazine. This compound was synthesized as previously reported.[1]

Synthesis of *N*-ethyl-3,7-dimethylphenothiazine. This compound was synthesized as previously reported.[2]

Synthesis of 3,7-dibromo-*N*-ethyl-phenothiazine. This intermediate was synthesized as previously reported.[2]

Synthesis of *N*-ethyl-3,7-dimethoxyphenothiazine (DMeOEPT). In a 25 mL round-bottomed flask immersed in an ice-water bath, a 5 M solution of sodium methoxide was prepared by dissolving sodium (0.25 g, 9.6 mmol) in methanol (2 mL) under nitrogen atmosphere. To the resultant solution, CuI (0.763 g, 4.01 mmol), 3,7-dibromo-*N*-ethyl-phenothiazine (0.383 g, 1.00 mmol), and anhydrous pyridine (5 mL) were added. The reaction mixture was sparged with nitrogen for 15 min. A reflux condenser was attached and the reaction was heated at 120 °C for 12 h. Upon completion of the reaction, the reaction mixture was diluted with diethyl ether and washed with brine. The organic extracts were dried over magnesium sulfate, filtered to remove solids, and concentrated by rotary evaporation. The organic residue was purified by silica-gel chromatography using 0-10% ethyl acetate in hexanes as eluent to afford the product as a white crystalline solid (0.264 g, 91%). ^1H NMR (DMSO-d_6, 400 MHz, ppm) δ 6.88-6.90 (m, 2H), 6.75-6.77 (m, 4H), 3.79 (q, J = 6.8 Hz, 2H), 3.69 (s, 6H), 3.33 (s, H_2O), 1.24 (t, J = 6.8 Hz, 3H). ^{13}C NMR (DMSO-d_6, 100 MHz, ppm) δ 154.5, 138.4, 124.3, 115.9, 112.9, 112.4, 55.4, 41.1, 12.8. GCMS: m/z 287 (41%), 258 (100%), 215 (18%). Anal. calcd. for $C_{16}H_{17}NO_2S$ C, 66.87; H, 5.96; N, 4.87. Found C, 66.70; H, 5.94; N, 4.95. Melting point: 115-116 °C. Crystals for X-ray diffraction were grown in a solution of methanol and water.

Synthesis of *N*-ethylphenothiazine tetrafluoroborate (EPT-BF_4). This compound was synthesized as previously reported.[3]

Synthesis of *N*-ethyl-3,7-dimethoxyphenothiazine tetrafluoroborate (DMeEPT-BF_4). 3,7-DMeEPT (0.12 g, 0.47 mmol) was dissolved in anhydrous dichloromethane (10 mL) in an oven-dried 50 mL round-bottomed flask fitted with a rubber septum and cooled under nitrogen. The resulting solution was purged with nitrogen for 10 min. Nitrosonium tetrafluoroborate (0.061 g, 0.52 mmol) was added to the solution, which immediately turned dark pink. The reaction vessel was capped and the reaction mixture stirred under nitrogen for 30 min, after which diethyl ether (20 mL) was added gradually with continued stirring, producing a dark precipitate. The precipitate was filtered, then dissolved in DCM (10 mL) and re-precipitated with diethyl ether (20 mL). This process was repeated once more to ensure removal of any unreacted starting material. The final precipitate was dried under vacuum (0.07 g, 44%) and stored in an argon-filled glovebox.

Synthesis of *N*-ethyl-3,7-dimethoxyphenothiazine tetrafluoroborate (DMeOEPT-BF_4). 3,7-DMeOEPT (2.12 g, 7.39 mmol) was dissolved in anhydrous acetonitrile (100 mL) in a 250 mL round-bottomed flask fitted with a rubber septum under nitrogen atmosphere. Nitrosonium tetrafluoroborate ($NOBF_4$, 0.798 g, 7.00 mmol) was added in a single portion, and the reaction was stirred at room temperature for 30 min. Upon completion, the reaction was concentrated under reduced pressure, producing a red solid. This solid was dissolved in dry acetone (ca. 40 mL) and cooled to 0 °C. Hexanes (200 mL) was added to precipitate the radical-cation salt, which was filtered and isolated. The precipitation and isolation procedure was repeated twice. The red solid was then dried under vacuum overnight to remove residual solvent, affording 1.47 g (56%) of product.

II. Nuclear Magnetic Resonance Spectroscopy

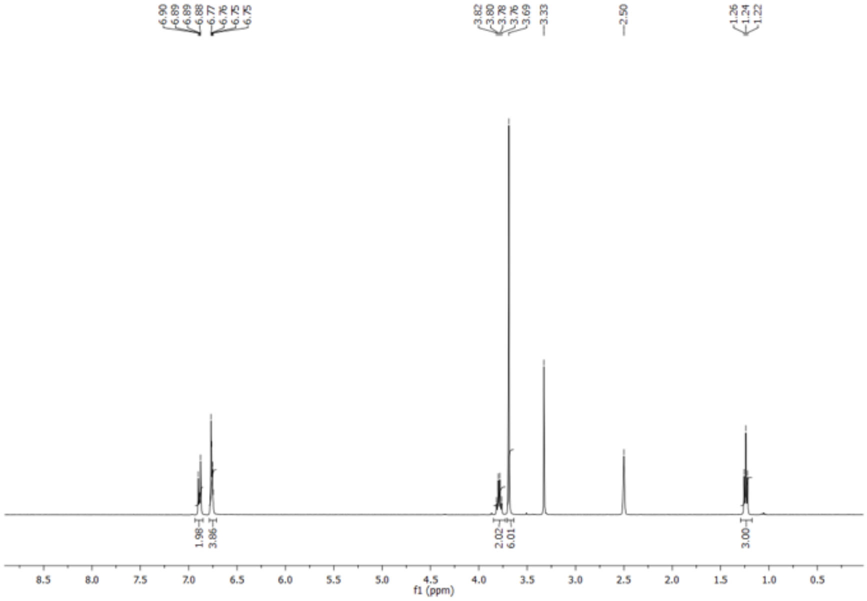

Figure S1. ^{1}H NMR spectrum of DMeOEPT in DMSO-d_6.

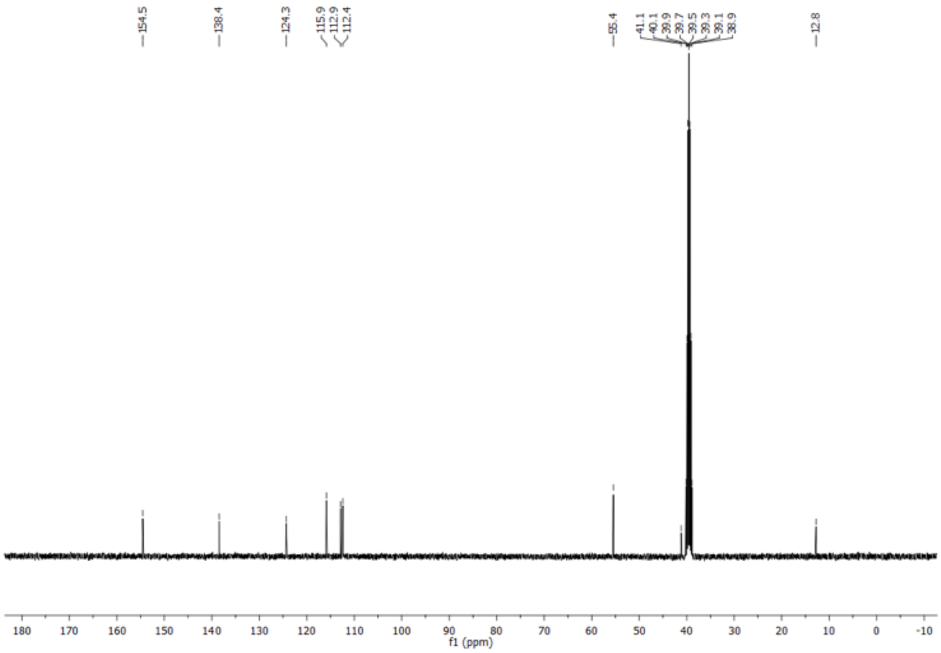

Figure S2. ^{13}C NMR spectrum of DMeOEPT in DMSO-d_6.

III. X-Ray Diffraction

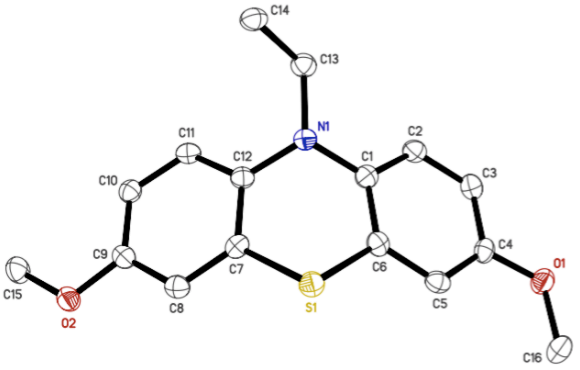

Figure S3. Thermal ellipsoid plot of DMeOEPT from single-crystal X-ray diffraction experiments.

IV. Spectroelectrochemistry

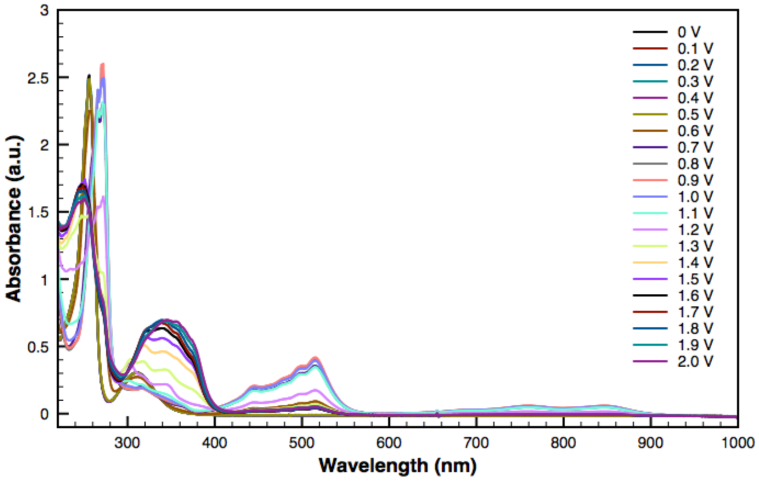

Figure S4. Spectroelectrochemistry of charging EPT. The radical cation and dication were generated by bulk electrolysis from solutions at 0.375 mM of active material.

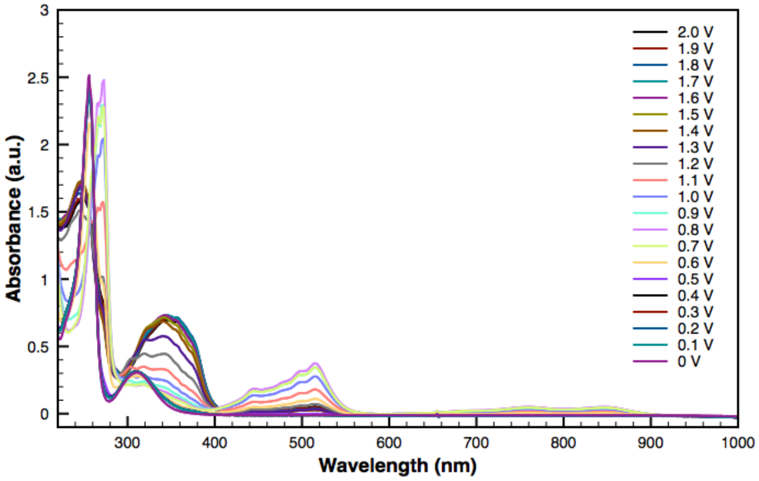

Figure S5. Spectroelectrochemistry of discharging EPT. The radical cation and dication were generated by bulk electrolysis from solutions at 0.375 mM of active material.

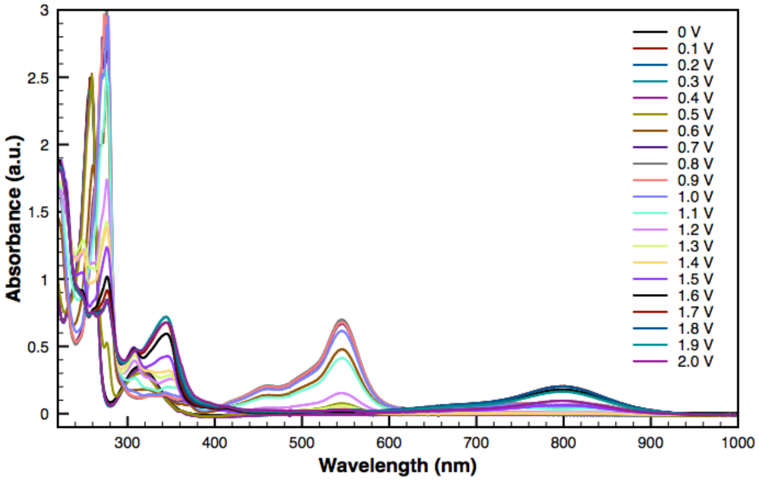

Figure S6. Spectroelectrochemistry of charging DMeEPT. The radical cation and dication were generated by bulk electrolysis from solutions at 0.375 mM of active material.

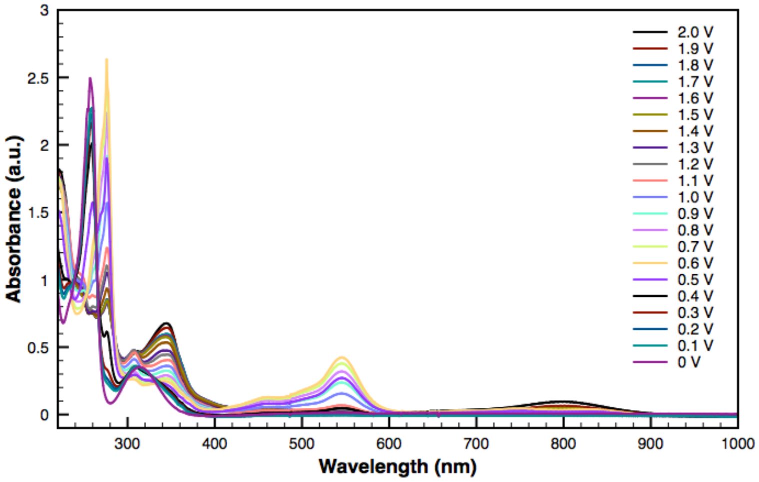

Figure S7. Spectroelectrochemistry of discharging DMeEPT. The radical cation and dication were generated by bulk electrolysis from solutions at 0.375 mM of active material.

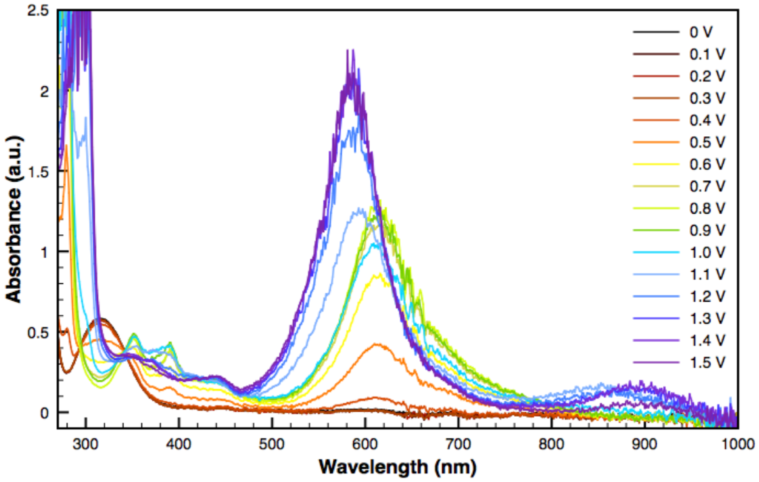

Figure S8. Spectroelectrochemistry of charging DMeOEPT. The radical cation and dication were generated by bulk electrolysis from solutions at 0.375 mM of active material.

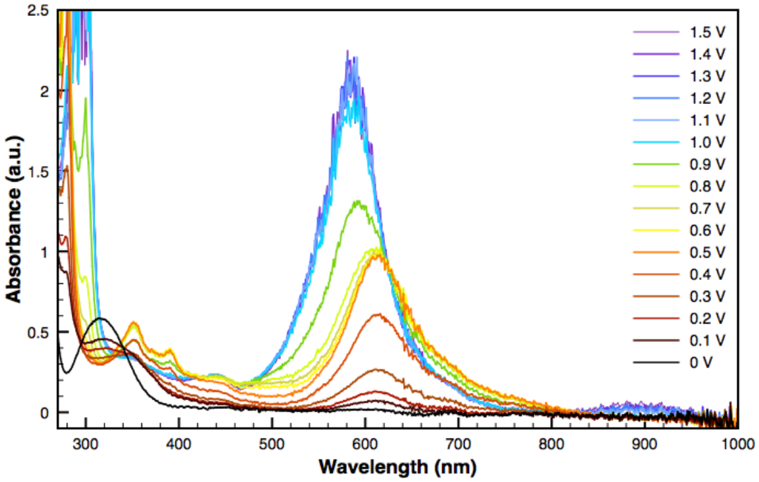

Figure S9. Spectroelectrochemistry of discharging DMeOEPT. The radical cation and dication were generated by bulk electrolysis from solutions at 0.375 mM of active material.

V. Density Functional Theory Calculations

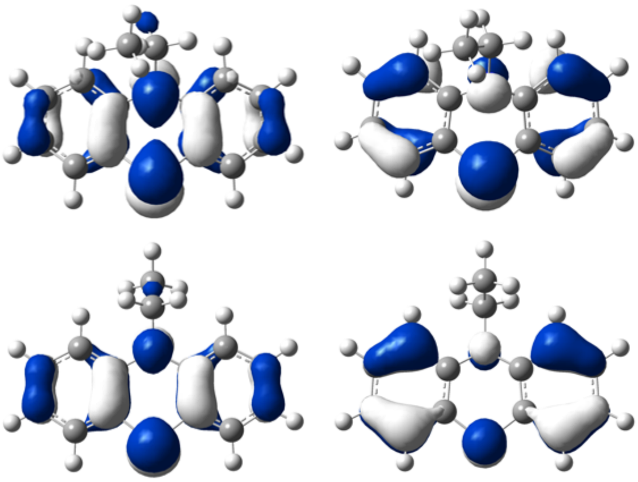

Figure S10. Pictorial representations of the EPT neutral highest occupied molecular orbital (HOMO) (top left) and HOMO-1 (top right); radical-cation singly occupied molecular orbital (SOMO) (bottom left); and dication HOMO (bottom right) as determined at the B3LYP/6-311G(d,p) level of theory.

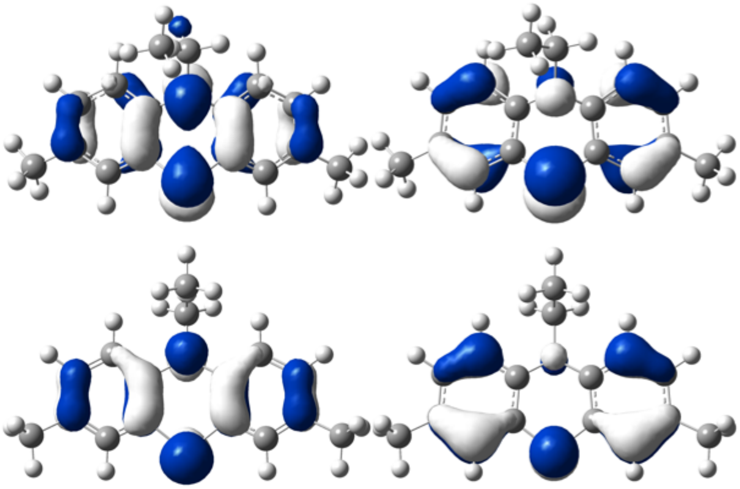

Figure S11. Pictorial representations of the DMeEPT neutral HOMO (top left) and HOMO-1 (top right); radical-cation SOMO (bottom left); and dication HOMO (bottom right) as determined at the B3LYP/6-311G(d,p) level of theory.

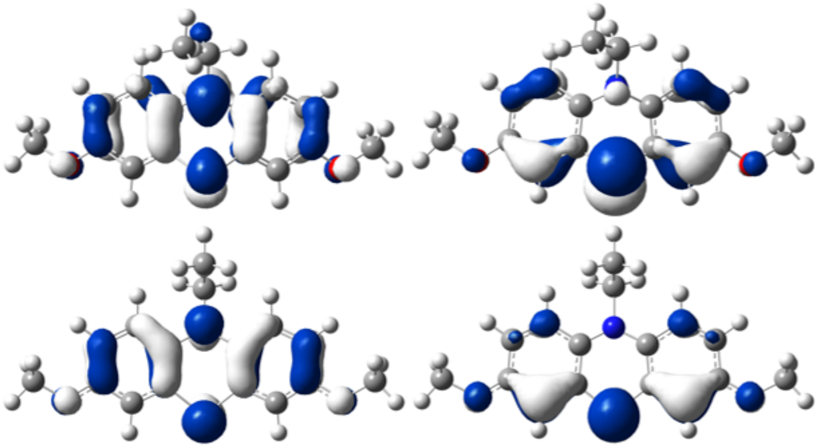

Figure S12. Pictorial representations of the DMeOEPT neutral HOMO (top left) and HOMO-1 (top right); radical-cation SOMO (bottom left); and dication HOMO (bottom right) as determined at the B3LYP/6-311G(d,p) level of theory.

Table S1. Mulliken charge distributions for dications of EPT and 3,7-disubstituted derivatives as determined at the B3LYP/6-311G(d,p) level of theory.

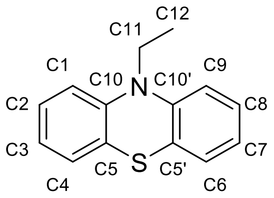

Atom / Atom Group	**EPT**	**DMeEPT**	**DMeOEPT**
C1-H	0.15	0.11	0.11
C2-H	0.15	0.16	0.11
C3-H	0.20	–	–
C3, CH_3	–	-0.09, 0.29	–
C3, O, CH_3	–	–	0.22, -0.27, 0.35
C4-H	0.15	0.16	0.14
C5	-0.26	-0.26	-0.25
C10	0.29	0.35	0.34
C9-H	0.15	0.11	0.11
C8-H	0.15	0.16	0.11
C7-H	0.20	–	–
C7, CH_3	–	-0.09, 0.29	–
C7, O, CH_3	–	–	0.22, -0.27, 0.35
C6-H	0.15	0.16	0.14
C5'	-0.25	-0.26	-0.25
C10'	0.29	0.35	0.34
N	-0.42	-0.46	-0.46
S	0.60	0.64	0.57
C11-H_2	0.22	0.17	0.16
C12-H_3	0.21	0.23	0.22

Table S2. Molecular lengths (Å) in the neutral, radical-cation, and dication forms of EPT and 3,7-disubstituted derivatives, measured between outermost H atoms (H-H distance) or between outermost C atoms *via* the internal N atom (C-N-C distance).

Molecule	Molecular Length (Å)					
	H-H Distance			C-N-C Distance		
	Neutral	Radical Cation	Dication	Neutral	Radical Cation	Dication
EPT	9.13	9.46	9.44	8.47	8.46	8.44
DMeEPT	11.08	11.54	11.43	11.53	11.52	11.47
DMeOEPT	13.18	13.83	13.83	12.95	12.94	12.96

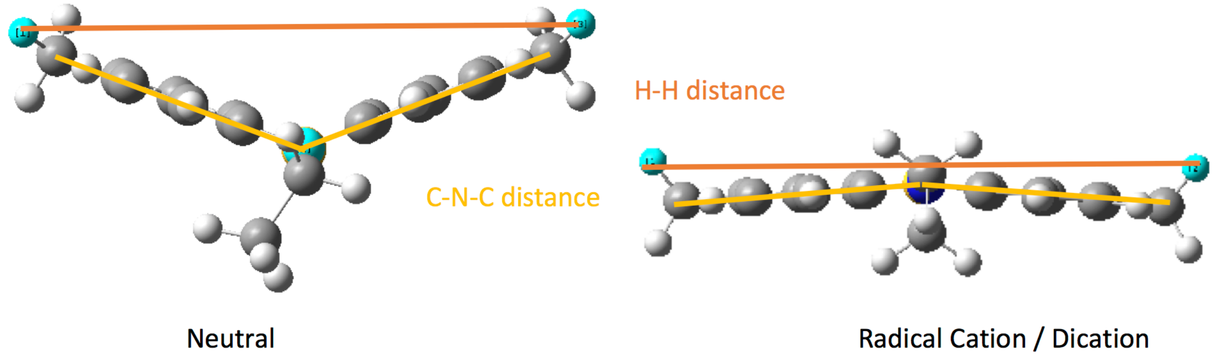

Figure S13. Drawings of how the H-H distance (orange) and C-N-C distance (yellow) were measured in the neutral and oxidized forms, showing DMeEPT as an example.

VI. Electrochemical Analysis

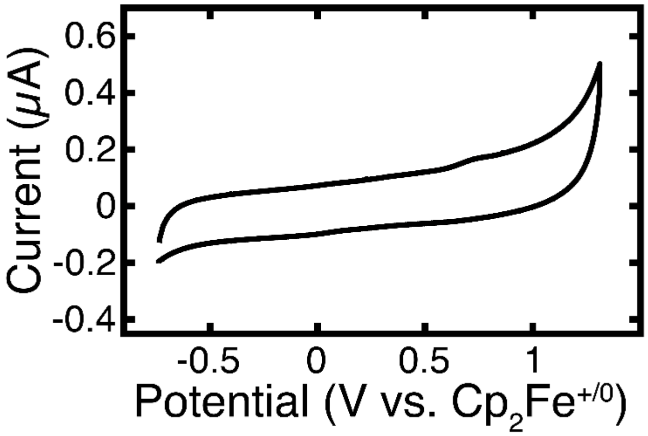

Figure S14. Background cyclic voltammogram of 1 M LiTFSI in PC recorded at a scan rate of 20 mV/s.

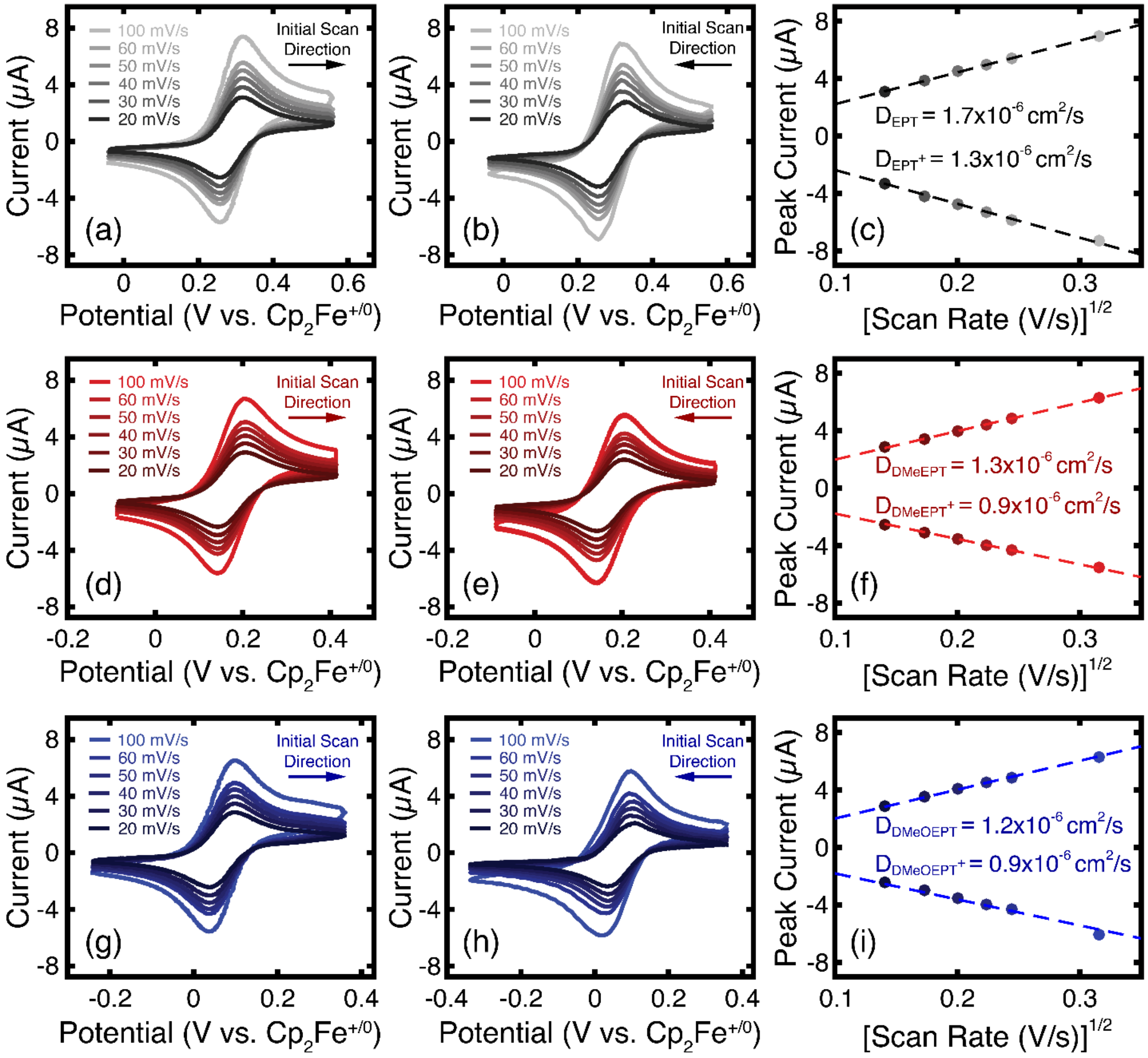

Figure S15. Cyclic voltammograms as a function of scan rate for EPT (a), EPT^+ (b), DMeEPT (d), $DMeEPT^+$ (e), DMeOEPT (g), $DMeOEPT^+$ (h), and the corresponding Randles-Sevcik peak-current analysis for EPT/EPT^+ (c), $DMeEPT/DMeEPT^+$ (f), and $DMeOEPT/DMeOEPT^+$ (i). All experiments were conducted with 1 mM active material in 1 M LiTFSI/PC.

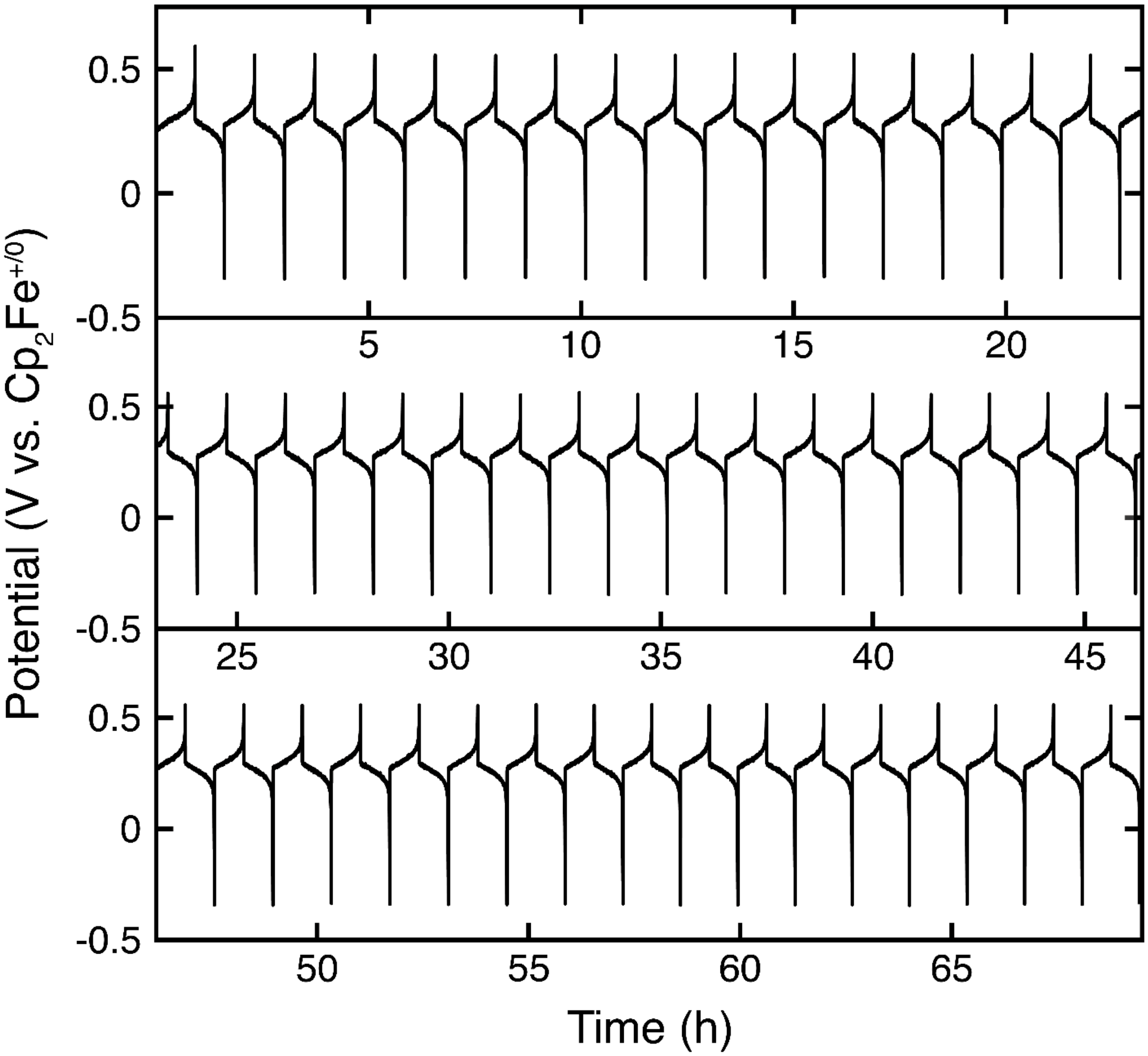

Figure S16. Complete voltage vs. time cycling profile of 1 mM EPT in 1 M LiTFSI/PC accessing only the first oxidation (50 cycles). The total solution volume was 30 mL, and the charge/discharge current was 0.804 mA.

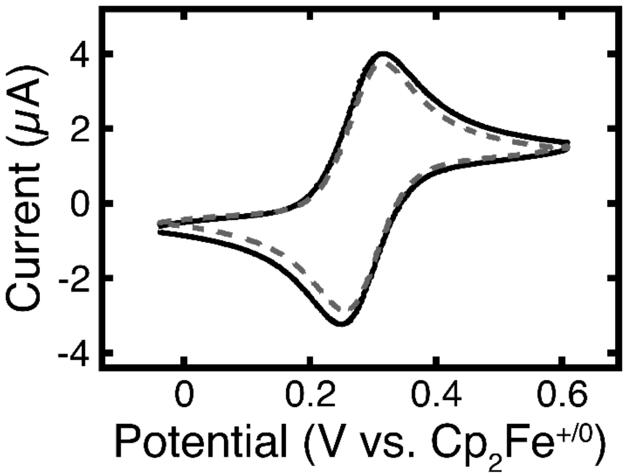

Figure S17. Cyclic voltammograms of 1 mM EPT in 1 M LiTFSI/PC before (solid line) and after (dashed line) 50 cycles of bulk electrolysis accessing only the first oxidation of EPT. Voltammograms were recorded at a scan rate of 20 mV/s.

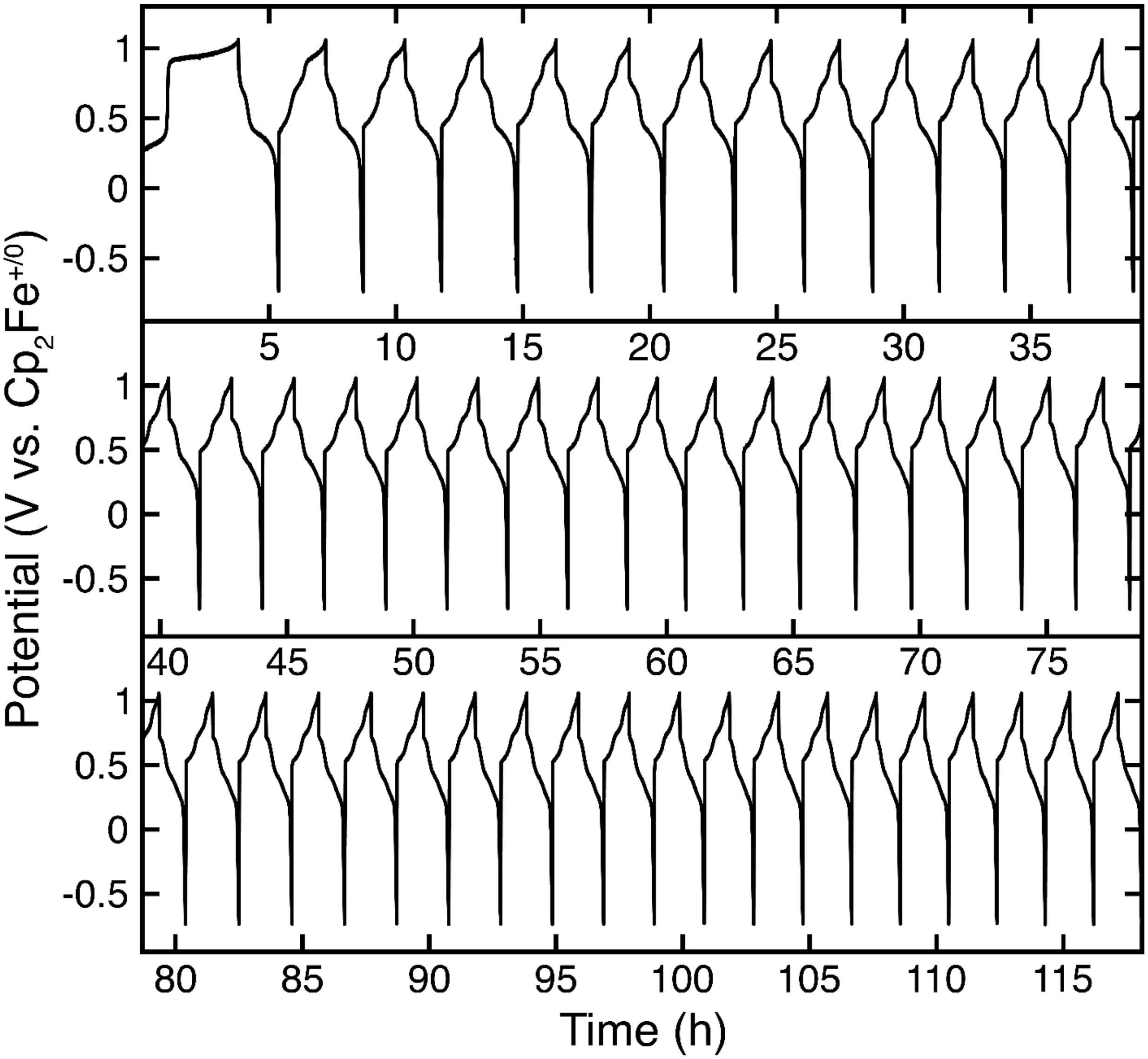

Figure S18. Complete voltage vs. time cycling profile of 1 mM EPT in 1 M LiTFSI/PC accessing both the first and second oxidations (50 cycles). The total solution volume was 30 mL, and the charge/discharge current was 0.804 mA.

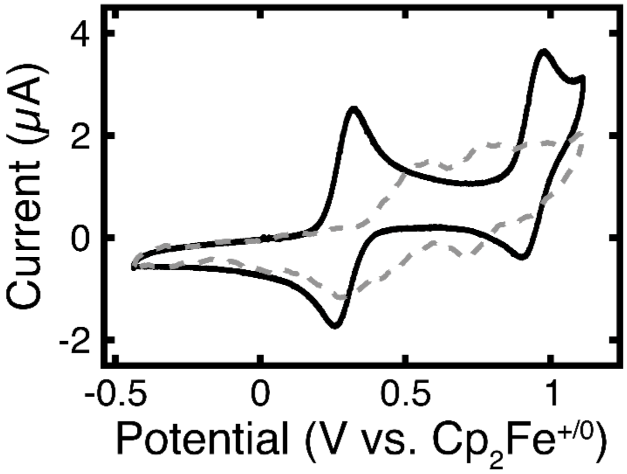

Figure S19. Cyclic voltammograms of 1 mM EPT in 1 M LiTFSI/PC before (solid line) and after (dashed line) 50 cycles of bulk electrolysis accessing both the first and second oxidations of EPT. Voltammograms were recorded at a scan rate of 20 mV/s.

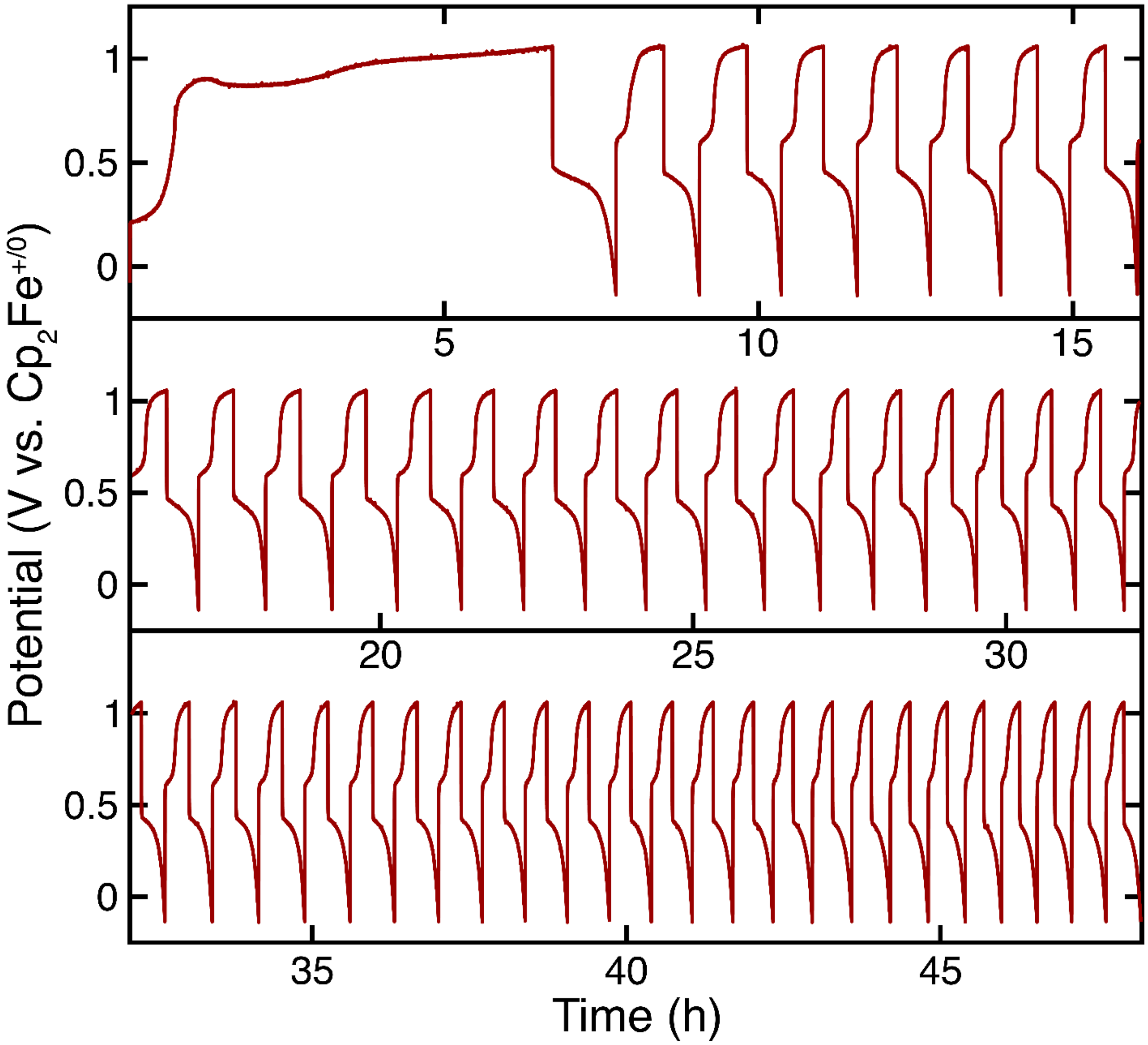

Figure S20. Complete voltage vs. time cycling profile of 1 mM DMeEPT in 1 M LiTFSI/PC accessing both the first and second oxidations (50 cycles). The total solution volume was 30 mL, and the charge/discharge current was 0.804 mA.

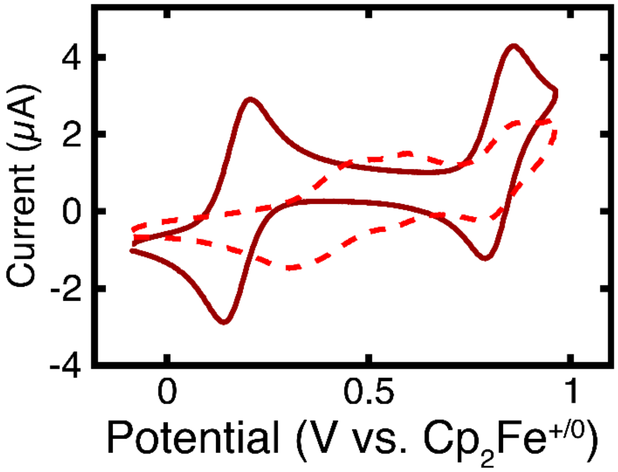

Figure S21. Cyclic voltammograms of 1 mM DMeEPT in 1 M LiTFSI/PC before (solid line) and after (dashed line) 50 cycles of bulk electrolysis accessing both the first and second oxidations of DMeEPT. Voltammograms were recorded at a scan rate of 20 mV/s.

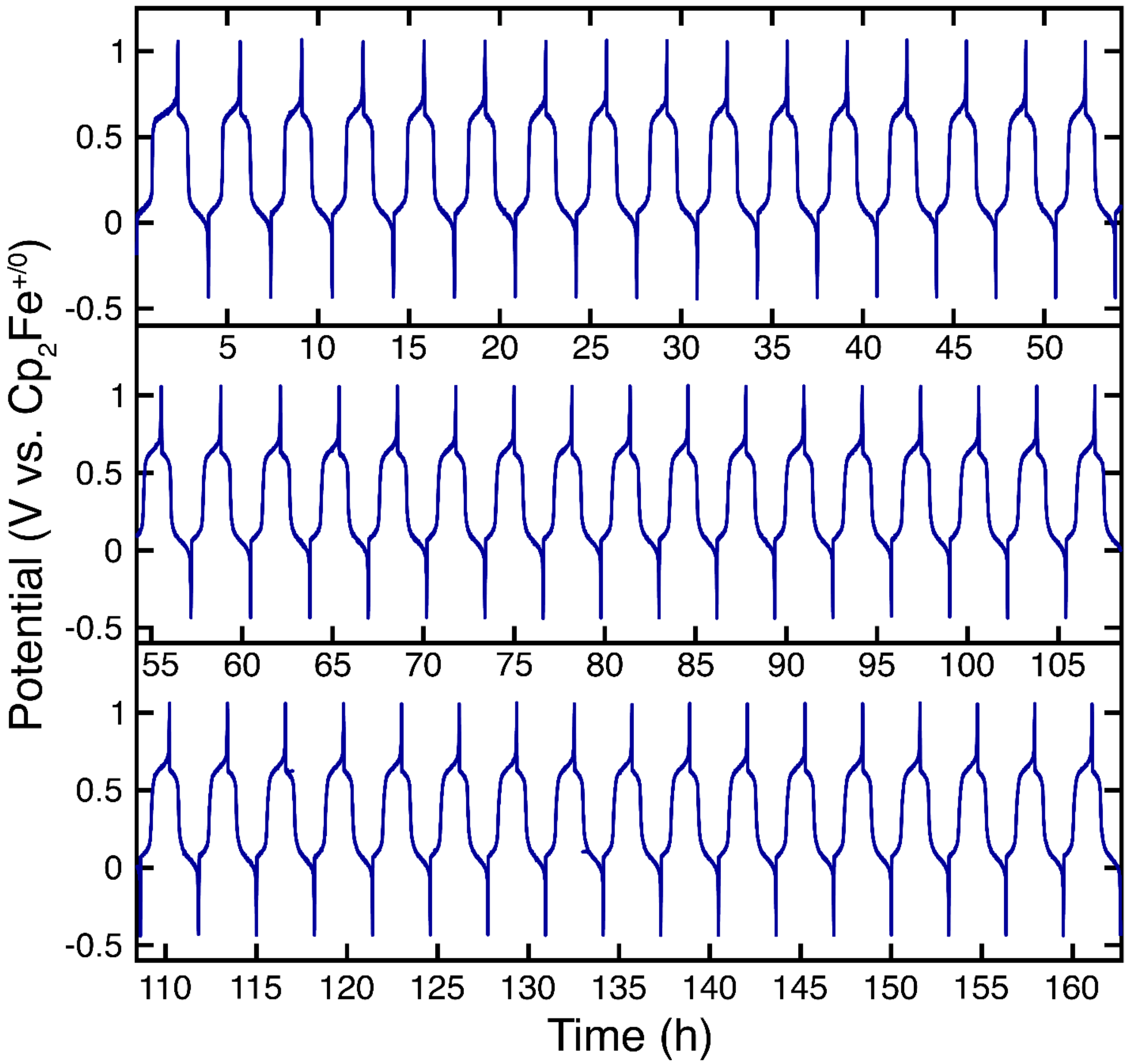

Figure S22. Complete voltage vs. time cycling profile of 1 mM DMeOEPT in 1 M LiTFSI/PC accessing both the first and second oxidations (50 cycles). The total solution volume was 30 mL and the charge/discharge current was 0.804 mA.

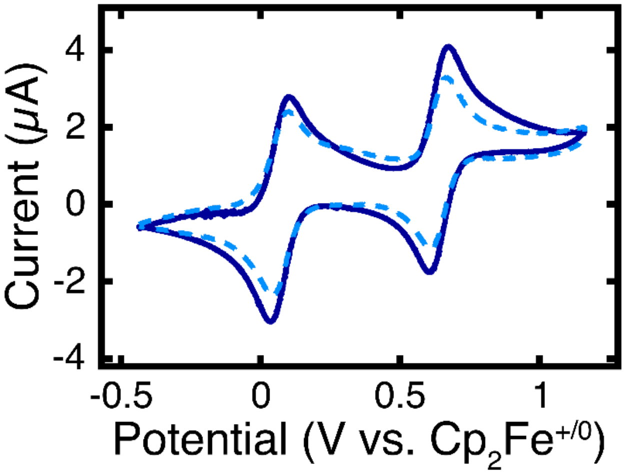

Figure S23. Cyclic voltammograms of 1 mM DMeOEPT in 1 M LiTFSI/PC before (solid line) and after (dashed line) 50 cycles of bulk electrolysis accessing both the first and second oxidations of DMeOEPT. Voltammograms were recorded at a scan rate of 20 mV/s.

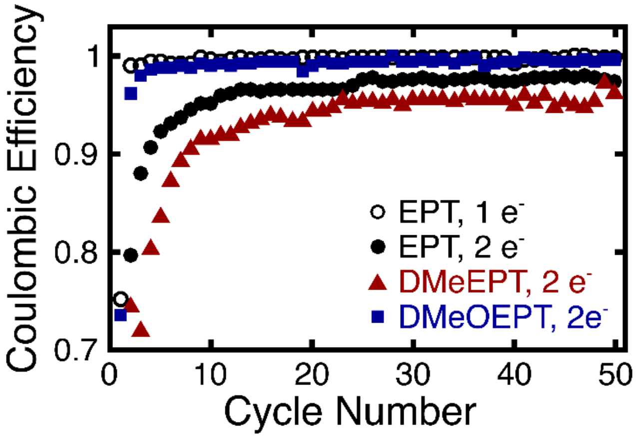

Figure S24. Coulombic efficiency vs. cycle number for bulk electrolysis charge/discharge experiments accessing the first oxidation of EPT (black, hollow circles), or both oxidations of EPT (black, filled circles), DMeEPT (red, filled triangles), or DMeOEPT (blue, filled square). For all experiments, the active species concentration was 1 mM in 1 M LiTFSI/PC (30 mL of solution), and the charge/discharge current was 0.804 mA.

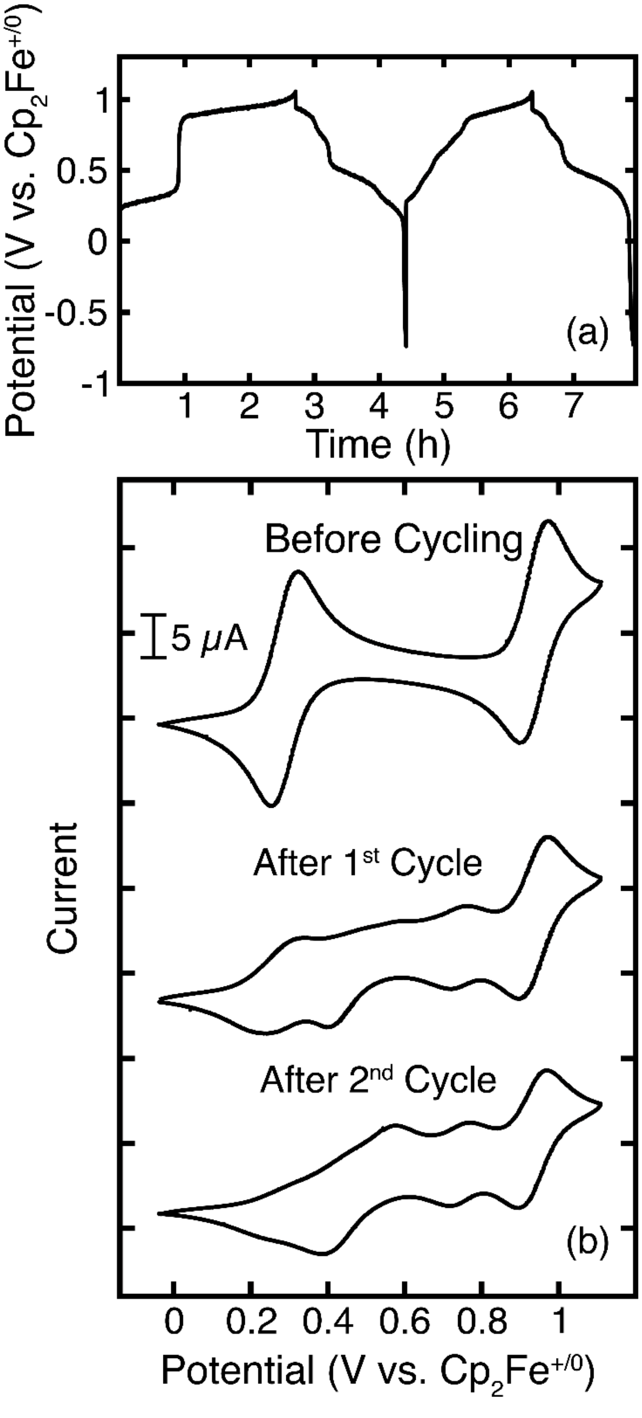

Figure S25. Voltage vs. time profile for the first two cycles of 5 mM EPT in 1 M LiTFSI/PC cycled through both oxidations (a). The charge/discharge current used was 0.469 mA and the solution volume was 3.5 mL. Cyclic voltammograms recorded before cycling (top), after the first complete cycle (middle), and after the second complete cycle (bottom) (b).

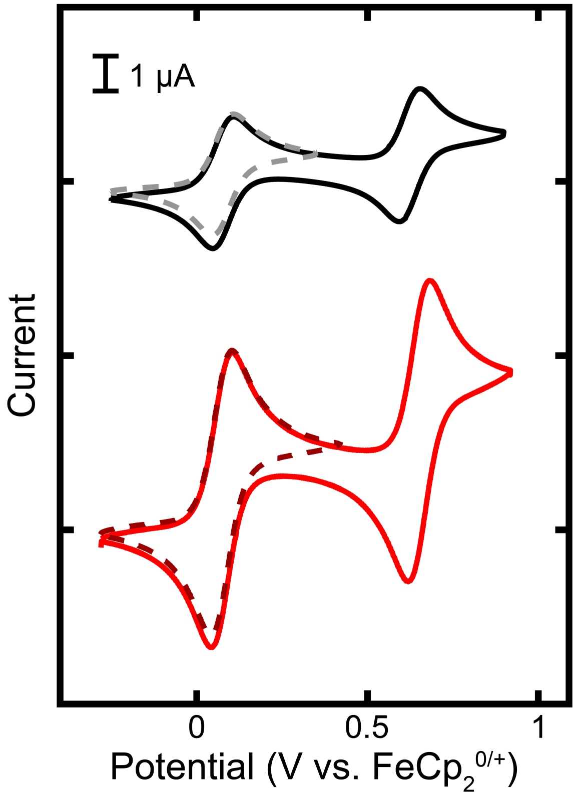

Figure S26. Cyclic voltammograms of the first and second oxidations of 1 mM DMeOEPT in 1 M $LiBF_4$ in PC (black, top) and 1 M $TBAPF_6$ in acetonitrile (red, bottom) at a scan rate of 10 mV/s. Solid lines depict CVs accessing both oxidation reactions, while dashed lines depict CVs accessing the first oxidation alone.

References

1. S. A. Odom, S. Ergun, P. P. Poudel and S. R. Parkin, *Energy Environ. Sci.*, 2014, **7**, 760-767.
2. S. Ergun, C. F. Elliott, A. P. Kaur, S. R. Parkin and S. A. Odom, *Chem. Commun.*, 2014, **50**, 5339-5341.
3. J. D. Milshtein, A. P. Kaur, M. D. Casselman, J. A. Kowalski, S. Modekrutti, P. Zhang, N. H. Attanayake, C. F. Elliott, S. R. Parkin, C. Risko, F. R. Brushett and S. A. Odom, *Energy Environ. Sci.*, 2016, **9**, 3531-3543.